We are IntechOpen,
the world's leading publisher of
Open Access books
Built by scientists, for scientists

5,900
Open access books available

145,000
International authors and editors

180M
Downloads

Our authors are among the

154
Countries delivered to

TOP 1%
most cited scientists

12.2%
Contributors from top 500 universities

CLARIVATE ANALYTICS
BOOK CITATION INDEX
INDEXED

WEB OF SCIENCE™

Selection of our books indexed in the Book Citation Index
in Web of Science™ Core Collection (BKCI)

Interested in publishing with us?
Contact book.department@intechopen.com

Numbers displayed above are based on latest data collected.
For more information visit www.intechopen.com

Developing High-Energy Dissipative Soliton 2 μm Tm³⁺-Doped Fiber Lasers

Yulong Tang, Chongyuan Huang and Jianqiu Xu

Additional information is available at the end of the chapter

Abstract

In recent years, mid-infrared (mid-IR) lasers have attracted a great interest over the world. During the development of mid-IR laser sources, the 2 μm Tm³⁺-doped fiber laser (TDFL) has played an important role for its specific emission wavelength between near-IR and mid-IR. Its great potential applications include sensing, medical surgery, ranging, telecommunications, and pump sources for developing 3–5 μm laser systems. Though the continuous-wave (CW) output power of 2 μm TDFLs has been scaled to over 1000 W, high-pulse-energy ultrafast 2 μm TDFLs are still limited by nonlinear optical effects. In traditional soliton mode-locking, the pulse energy has an upper limit defined by the soliton area theorem (or energy quantization principle). For improving the pulse energy of 2 μm fiber lasers, dissipative soliton (DS) mode-locking may be one of the efficient solutions. In this chapter, the current state of the art in high-energy ultrafast DS 2 μm TDFLs developed in our laboratory is reviewed, and the potential and prospect of this theme are analyzed. By introducing a new model, condensed-gain fiber mode-locking, we show that the soliton pulse energy of 2 μm TDFLs can be steadily scaled to over 10 nJ and various soliton dynamics (harmonic mode-locking, soliton molecules, etc.) can be observed. Furthermore, DS mode-locking of TDFLs with one of the two-dimension-like materials (MoS_2) is investigated.

Keywords: dissipative soliton, high pulse energy, Tm³⁺-doped fiber laser, mode-locking, ultrafast fiber laser

1. Introduction

In recent years, ultrafast 2 μm fiber lasers have attracted considerable attention around the world and have found extensive application in areas like LIDAR, surgical operation, molecule

spectroscopy, optical sensing, medical treatment, material processing, and nonlinear microscopy [1–8]. In application, ultrashort pulses are usually required to have high pulse energy, which is very important for both scientific and industrial aims. In addition, achieving high energy short pulses at various wavelengths is the persistent pursuit of laser scientists.

Compared to traditional solid-state lasers (SSLs), fiber lasers (FLs) are better candidates for generation of ultrashort laser pulses due to their advantages of compactness, robustness, and good laser beam quality. Conventionally, generation of short pulses from fiber systems is achieved by the soliton mode-locking mechanism. Various passive mode-locking techniques can be employed, including the nonlinear polarization rotation (NPR) [9, 10], the nonlinear loop mirror [11, 12], and the saturable absorber method [13, 14]. However, pulse energy of traditional solitons (with anomalous net cavity dispersion), which is based on the balance of dispersion and nonlinearity, is usually limited by the soliton area theorem [15, 16] or the pulse peak power clamping effect [17, 18] to less than 1 nJ. Therefore, fiber lasers still produce much lower pulse energy than their solid-state counterparts [19].

To improve the pulse energy of fiber lasers, many techniques have been proposed and explored [20–36], among which four kinds of mechanisms have played important roles: dispersion-managed soliton [20–22, 37, 38], all normal dispersion mode-locking [39], self-similar soliton [27–30], and dissipative soliton (DS) [31–36]. By taking advantage of the balance between not only nonlinearity and dispersion but also gain and loss, DS mode-locked fiber lasers have realized pulse energy 1–2 orders of magnitude larger than those from conventional soliton mode-locking [31, 32]. However, although the DS pulse energy from 1 to 1.5 μm fiber lasers has exceeded 10 nJ [40–42] and even over 20 nJ [33–35], pulse energy of 2 μm DS fiber lasers still remains at a low level. This is because the currently available gain fibers (GFs) in the 2 μm region show relatively large anomalous dispersion, resulting in conventional soliton mode-locking operation of 2 μm fiber lasers [43–48]. Therefore, the pulse energy is still governed by the soliton area theorem and clamped by peak power [15, 17].

DS mode-locking has been widely adopted as an efficient method to improve the pulse energy of 2 μm fiber lasers. To implement DS mode-locking, the whole cavity's dispersion has to be pushed into the normal dispersion region. To that end, various methods have been proposed, e.g., inserting a chirped fiber Bragg grating into the cavity to provide normal dispersion [49] or incorporating specially designed dispersion-compensating fibers (DCFs) into the cavity [50–52]. However, these methods only improve pulse energy to around 1 nJ, and the great potential of DS mode-locking mechanism has not been fully explored.

Here, we will first present a new model to investigate the intracavity pulsing dynamics of a 2 μm DS mode-locked fiber laser and show that (different from the 1 to 1.5 μm counterparts) the pulse energy of 2 μm DS fiber lasers is mainly limited by the nonlinear phase shift caused by the gain fiber, and thereafter we propose that the anomalous dispersive GF should be condensed as short as possible to efficiently decouple gain from dispersion and nonlinearity. We name it the condensed-gain fiber mode-locking (CGFML). By avoiding too much phase accumulation, numerical simulations show that over 10 nJ DSs at 2 μm are readily feasible. After that, we carry out experimental operation of such CGFML of a 2 μm fiber laser, and a 4.9 nJ DS with 579 fs dechirped pulse duration is achieved. By further optimizing the cavity, the pulse

energy of such mode-locked fiber laser can be improved to over 12 nJ, which is comparable to that of conventional solid-state mode-locked lasers. Under high pumping levels, pulsing dynamics of the CGFML fiber laser are studied, and high-energy harmonic mode-locking is realized. Finally, we present high-energy mode-locking of 2 μm fiber laser with new developed 2D materials (MoS2) and also achieve over 15 nJ pulse energy. These research results indicate that the CGFML is a new route to develop high-energy fiber lasers with short pulse duration in the 2 μm wavelength region.

2. Condensed-gain dissipative soliton model and simulation for 2 μm fiber lasers

Based on detailed simulation of the dynamics of short pulse propagating in various fiber circumstances, we found that the main factor that limited the pulse energy in 2 μm DS fiber lasers was related with nonlinear phase shift, which was primarily accumulated in the gain fiber. If we can efficiently control the nonlinear phase shift generated in the gain fiber, then the pulse energy of 2 μm DS fiber lasers probably can be significantly scaled. Therefore, we propose a condensed-gain fiber model where the gain fiber should be shortened as much as possible, and in the following, we give a detailed description about the model and carry out simulation about the pulse dynamics happened in a 2 μm DS fiber laser.

A simple schematic diagram for the CGFML model is shown in **Figure 1(a)** [53]. The fiber laser cavity mainly includes five elements: output coupler (OC), single-mode fiber (SMF), gain fiber (GF), dispersion-compensating fiber (DCF), and saturable absorber (SA). Here, we use a single-mode highly doped 2 μm thulium fiber as the GF. Light evolution (pulse shape, pulse intensity, and spectrum) in the laser cavity is traced through solving the well-known nonlinear Schrodinger equation (NLSE) [27], which needs the original equation:
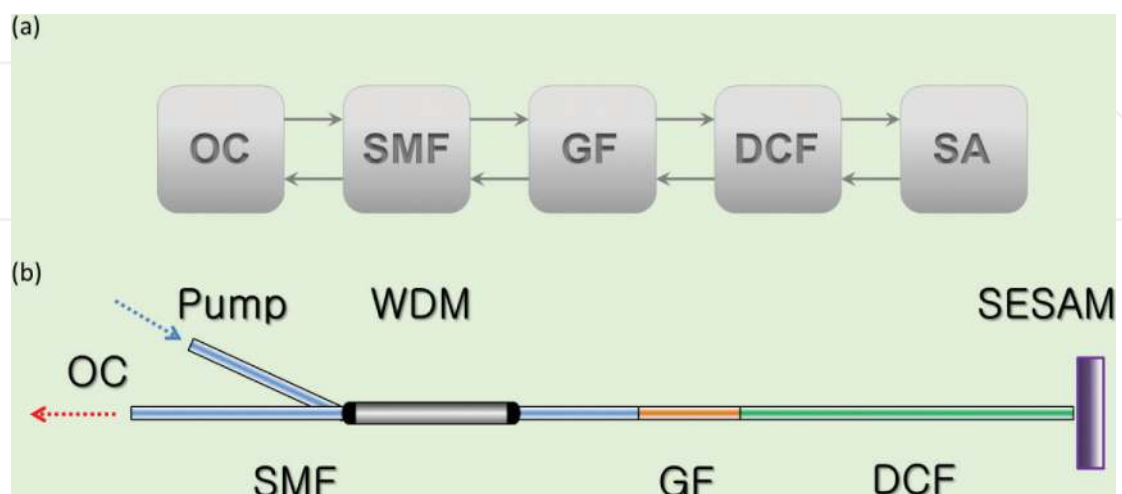

Figure 1. (a) Schematic diagram of the condensed-gain fiber laser model shows the light flow in the cavity. (b) Experimental setup of the SESAM mode-locked fiber laser system with a linear cavity. OC, output coupler; SMF, single-mode fiber; GF, gain fiber; DCF, dispersion-compensating fiber; SA, saturable absorber [53].

$$\frac{\partial U(z,\tau)}{\partial z} + i\frac{\beta_2}{2}\frac{\partial^2 U(z,\tau)}{\partial \tau^2} = i\gamma \left| U(z,\tau) \right|^2 U(z,\tau) + gU(z,\tau) \tag{1}$$

where $U(z,\tau)$ is the envelope of the light field, z is the propagation coordinate, and τ is the time-delay parameter. The SMF (8.2/125 μm, 0.14 NA) has a length of 1.4 m, with $\beta_2 = -67$ ps^2/km and $\gamma = 0.001$ (Wm)$^{-1}$, while the DCF (2.2/125 μm, 0.35 NA) is 1.5 m long with $\beta_2 = 93$ ps^2/km and $\gamma = 0.007$ (Wm)$^{-1}$, respectively. The 0.2 m GF (5/125 μm, 0.24 NA), with $\beta_2 = -12$ ps^2/km and $\gamma = 0.003$ (Wm)$^{-1}$, has the gain (including saturation) as.

$$g = g_0 / \left[1 + E_{pulse}/E_{sat} + (\omega - \omega_0)^2/\Delta\omega^2 \right] \tag{2}$$

where g_0 is the small-signal gain (here it is taken to be 30 dB), E_{pulse} is the pulse energy, E_{sat} is the gain saturation energy, ω_0 is the gain-center angular frequency, and $\Delta\omega$ is the gain bandwidth (assume 90 nm).

The saturable absorption effect of SA is included by using the transfer function:

$$T = 1 - l_0 / \left[1 + P(\tau)/P_{sat} \right] \tag{3}$$

where l_0 is the unsaturated loss (take 0.7), $P(\tau)$ is the instantaneous power, and P_{sat} is the saturation power. A critical factor for achieving DS is that spectral filtering is required to balance gain and loss. To that end, a 150-nm-bandwidth spectral filter (SF) is exerted on the SA.

Here, the split-step Fourier method is used to solve the NLSE. Simulation is started as the following procedure. With an initial white noise, the light is calculated in both temporal and spatial regions until a steady state is reached. The pump level and saturable effect are controlled through changing the values of E_{sat} and P_{sat}. When we take $P_{sat} = 3.5$ kW and $E_{sat} = 3.4$ nJ, the pulse's temporal and spectral evolution characteristics are shown in **Figure 2** [53]. In this case, the stable solution of pulse energy is 5 nJ. Detailed variations of pulse shape/width and spectral shape are clearly shown. In the DCF, owing to the combined effects of normal group velocity dispersion (GVD) and nonlinearity (NL), the pulse propagates with its duration increasing monotonically. The broadened pulse is then compressed by the SMF and GF with anomalous GVD. The pulse's spectrum has steep edges, and the bandwidth negligibly changes during the pulse circulating inside the cavity. However, the spectrum shape shows characteristic changes during the pulse evolution. The GF tends to amplify the spectrum's center more, and thus, the spectrum top becomes more arched. At the same time, the amplified pulse gives rise to increased self-phase modulation, thus leading to sharp edge peaks of the spectrum. Then, after being successively shaped by SA, DCF, GF, and SMF, the spectrum recovers its nearly flat-top shape. We can also see the advantages of the condensed-gain fiber model from the phase shift during the pulse evolution. As shown in **Figure 2(b)** [53], after passing through the three different kinds of fibers (DCF, GF, and SMF), very little phase shift is accumulated by the GF, which is finally compensated by both the DCF and the SMF.

To gain deeper insight into the intracavity pulsing dynamics, a qualitative illustration for 2 μm DSs is summarized in **Figure 3** [53], along with their 1 and 1.5 μm counterparts (insets) [54].
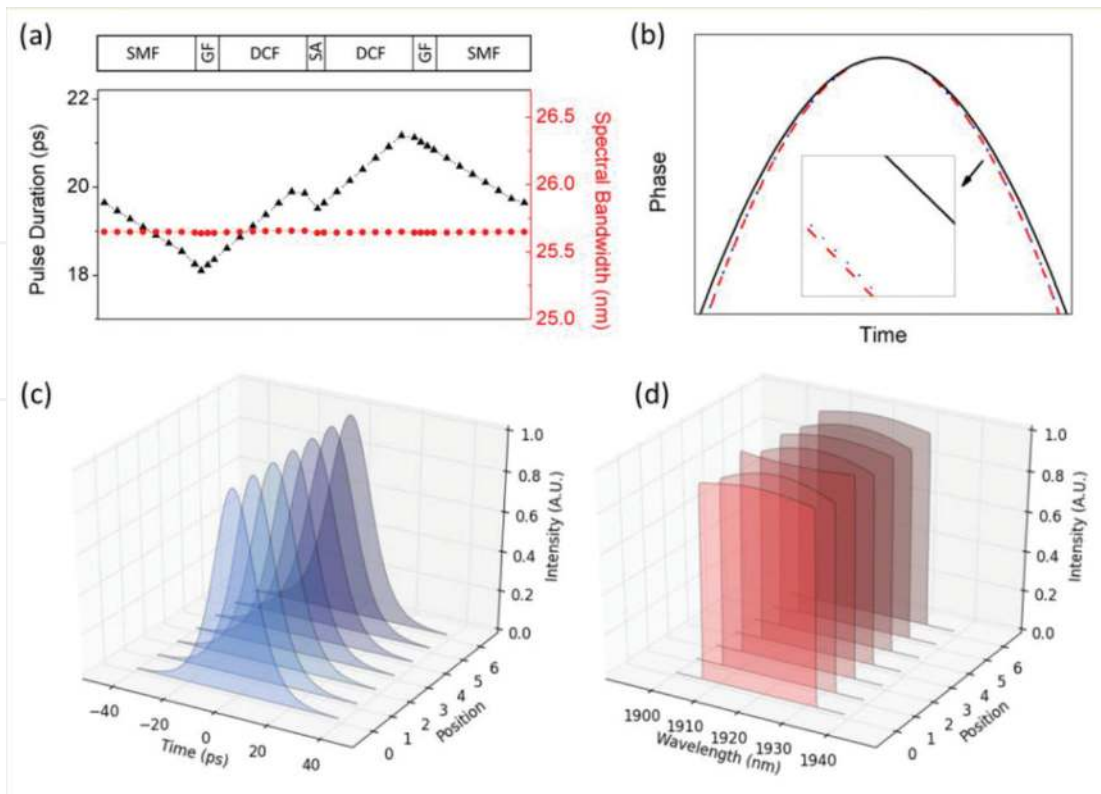
Figure 2. Evolution dynamics of pulse duration (black triangles) and spectral bandwidth (red circles) through different elements inside the laser cavity (a) and temporal phase of the pulse after DCF (black solid), GF (red dashed), and SMF (blue dotted) (b) and temporal (c) and spectral profiles (d) of the pulse after successive elements [53].
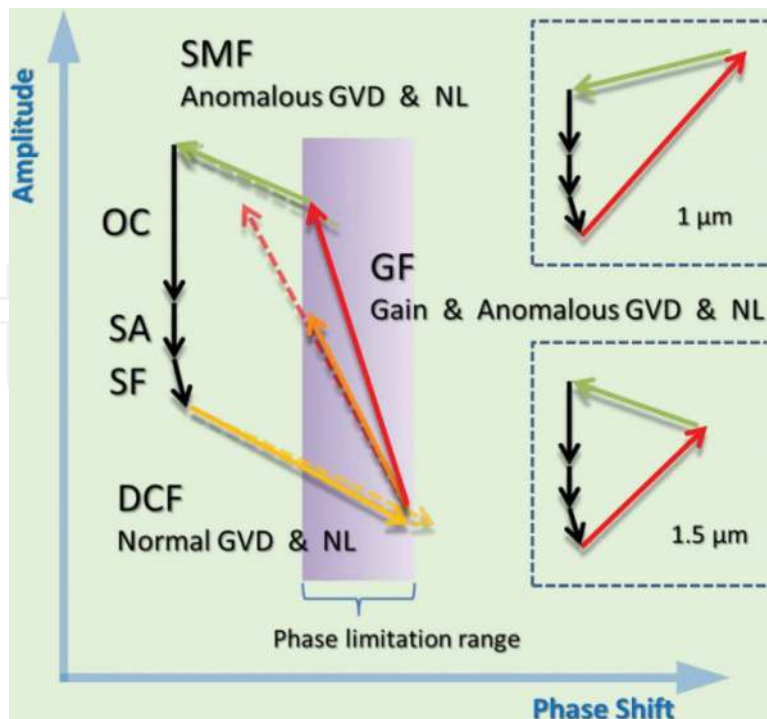

Figure 3. Schematic diagram for the amplitude and phase balances in a 2 μm fiber laser (insets show the counterparts of 1 μm and 1.5 μm systems) [53].

As shown in the insets, in the case of 1 and 1.5 μm, the GFs (Yb-doped or Er-doped) have normal dispersion and introduce positive phase shift, which can be compensated (even if the shift is large) by the negative phase shift provided by the SMF. However, it is quite different in the 2 μm wavelength regime, where the GF (Tm-doped) has anomalous dispersion and, thus, negative phase shift. To achieve soliton mode-locking, normally dispersive fibers (DCF and SMF) are thus required to be integrated into the cavity. However, too large normal dispersion value (long fibers) will induce large phase shift and consequently pulse splitting. Therefore, small net normal dispersion (caused both by DCF and SMF) places a tolerant phase shift region for the GF (purple area). A longer GF will induce much more significant phase shift (red-dashed arrow) than that incurred by the DCF or SMF (yellow- or green-dashed arrow). In the phase limitation range, shorter GF (red arrow) has a larger slope and hence can achieve higher pulse energy. On the contrary, longer GF (orange arrow), due to its smaller slope, has to sacrifice a large part of amplitude to reduce its phase shift under the tolerable level. Therefore, short GF should be adopted to achieve high energy pulses from a cavity in the 2 μm spectral region.

Based on the above analysis, we propose the condensed GF (shortened to a small length while providing adequate gain at the same time) to scale the pulse energy of DSs in the 2 μm and mid-infrared spectral regions. Within the phase limitation range, a condensed GF has a large slope (**Figure 3** [53]) and thereby can provide high pulse energy.

To verify the advantages of CGFML in the 2 μm regime, we carry out simulations in a semiconductor saturable absorber mirror (SESAM) mode-locked fiber laser (**Figure 1** [53]). The simulated maximum output pulse energies with various GF lengths are indicated in **Figure 4(a)** [53]. It is clear that decreasing the GF length will dramatically increase the pulse energy. Shortening the GF to 0.2 m, as high as 11 nJ pulses, is achieved, which is much higher than the pulse energy of tradition solitons (usually less than 1 nJ). This thus confirms that CGFML is an effective route for generating high-energy soliton pulses in laser systems with anomalous dispersion GFs (shortening the anomalous dispersion GF as much as possible).

3. High-energy dissipative soliton 2 μm fiber lasers

To verify the simulation results, we carried out a corresponding experimental observation of 2 μm DS mode-locking with short GFs. These GFs are highly thulium doped, and the net cavity dispersion is kept normal through adjusting the length of the DCF and SMF. Experimental setup is schematically shown in **Figure 1(b)** [53]. The pump source is a 1550-nm-CW Er/Yb-codoped fiber laser with maximum output of 1 W. The pump light is delivered into the gain fiber (with absorption of ~1.2 dB/cm at 1550 nm) by wavelength-division-multiplexing (WDM) couplers with a coupling efficiency of 95%. The parameters of these three kinds of fibers are the same as used in the simulation. Total cavity dispersion is kept at a net normal value of ~0.04 ps^2. On the output end, the perpendicularly cleaved fiber facet is employed for both laser feedback (~4% Fresnel reflection) and the output coupler (~96% output coupling ratio). The right side fiber end is directly butt coupled to the SESAM with a reflectance of ~85% at 1900 nm, a modulation depth of ~25%, and a saturation fluence of ~35 mJ/cm^2.

Short lengths of single-cladding Tm-doped fiber (tens of centimeters) are chosen as the GF. Under stable mode-locking operation, maximum pulse energies with different GF lengths are shown in **Figure 4(b)** [53]. The experimental results clearly follow the trend of the simulation prediction; that is, the pulse energy increases quickly as the length of GF decreases. When the GF length is shortened to ~15 cm, pulse energy of ~5 nJ is achieved, and detailed laser characteristics are shown in the following.

With the 15 cm GF, stable CW mode-locking is self-started when pump power is increased to ~650 mW. Owing to the large output coupling ratio suppressing the intermediate transitions between the CW laser operation and the CW mode-locking regime [55], no Q-switching or Q-switched mode-locking is observed. The stable CW mode-locked operation maintains when pump power is increased up to the maximum 1 W available pump power. The maximum average output power of this 2 µm DS fiber laser is 158 mW. **Figure 5(a)** [53] shows the 2 µm DS pulse train at the maximum output. The repetition rate is ~32 MHz, giving a pulse energy of ~4.9 nJ.

The laser spectrum, detected with a spectrometer (0.1 nm resolution), is shown in **Figure 5(b)**. The center wavelength is 1918 nm and the 3 dB bandwidth is 15 nm. Steep spectral edges indicate the typical characteristics of DSs [31, 32]. The radio-frequency (RF) spectrum (**Figure 5(c)**) has a signal-to-noise ratio of ~52 dB, showing that the mode-locking state is very stable. We also use an autocorrelator to measure the pulse characteristics at the maximum output, and the pulse shape (autocorrelation (AC) trace) directly outputted from the laser cavity is indicated in **Figure 5(d)**. The autocorrelation trace is fitted well by a Gaussian curve, giving a pulse duration of 16 ps. Therefore, the time-bandwidth product of the 2 µm DS pulse is calculated to be 18, which is highly chirped. For compressing this chirped pulse, we couple the output pulse directly into a ~25 m length of SMF-28 fiber. After dispersion compensation, the pulse is compressed to 579 fs (**Figure 5(e)**), and the time-bandwidth product reduces to 0.7.

This CGFML model can be readily extended to beyond 2 µm, e.g., mid-infrared fiber lasers to scale DS energy. According to this model, to achieve high-energy DSs, the GF length should
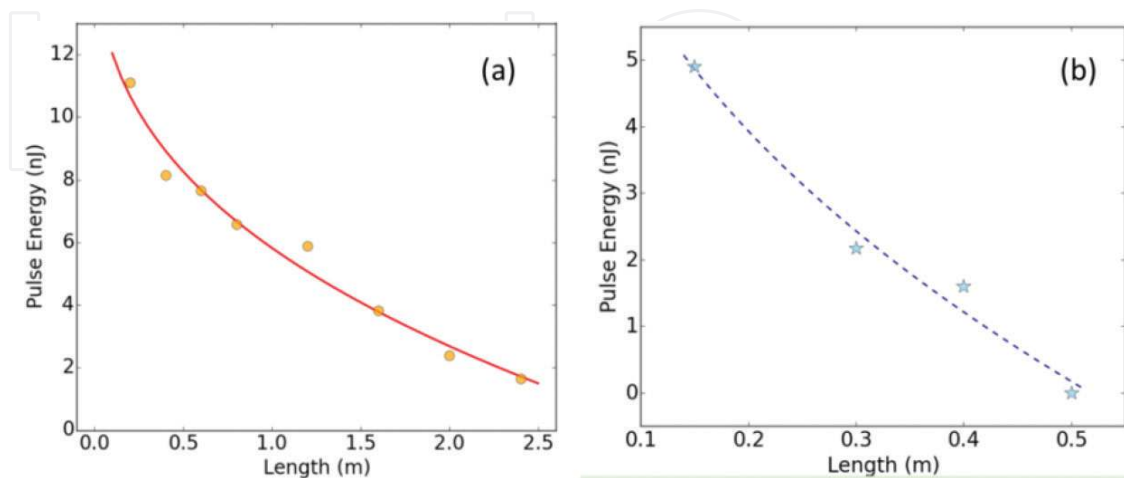

Figure 4. Simulated (circle dots) (a) and measured (asterisk dots) (b) maximum pulse energy under different lengths of GF under the pump power of 1 W. The curves are exponential fittings [53].
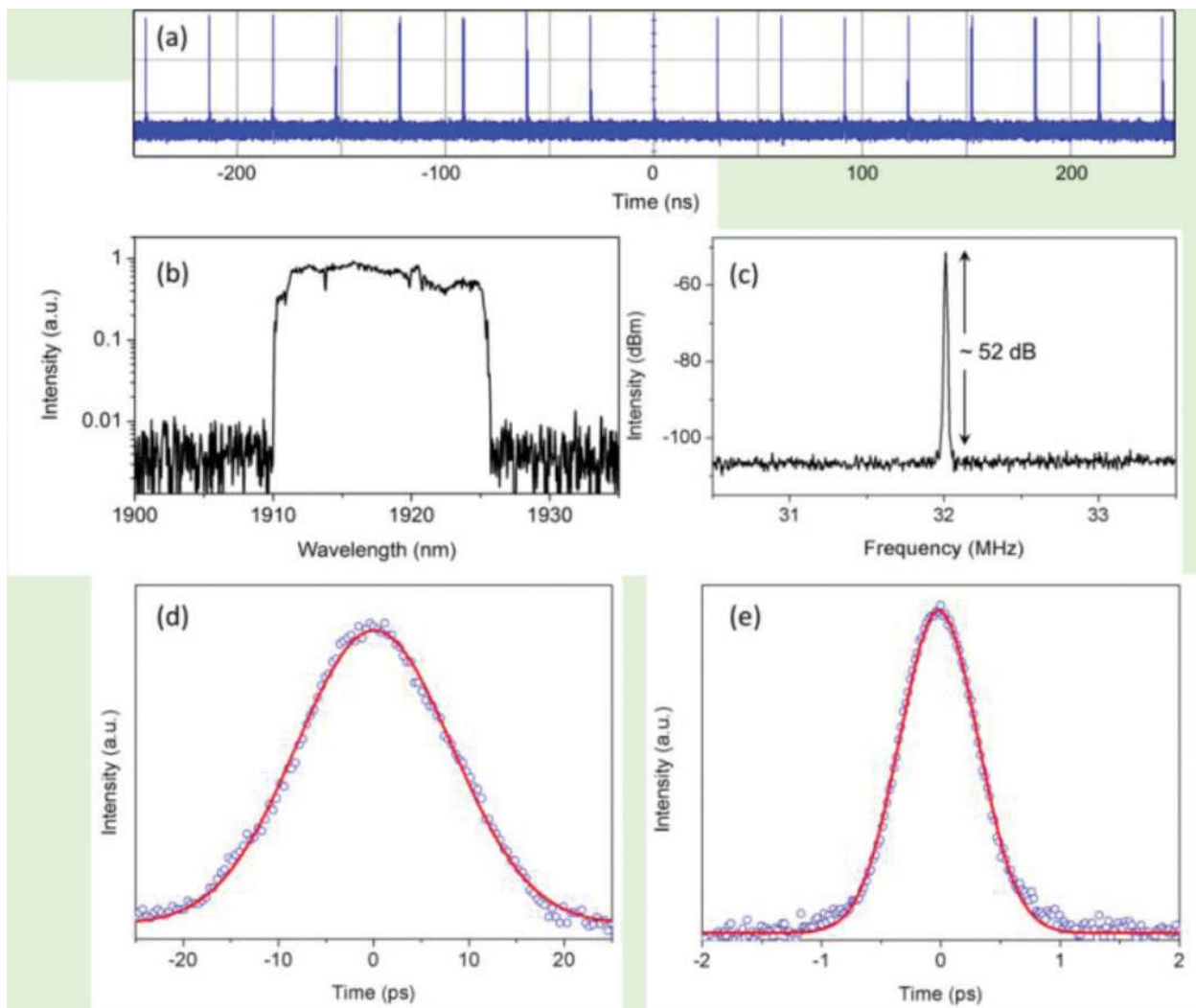
Figure 5. The laser pulse train (a), laser spectrum (b), and RF spectrum (c) of the mode-locked Tm-doped fiber laser and the autocorrelation traces of the pulse before (d) and after (e) dispersion compensation [53].

be as short as possible to keep phase shift within the phase limitation range while providing enough gain at the same time. To this end, the GF should be highly doped (short length with enough gain), so that gain can decouple from dispersion and suppress phase shift. This can efficiently avoid the pulses' evolution to conventional solitons during amplification in the GF. This CGFML model can also be applied for ring laser cavities. In a ring cavity, the pulse passes every element only once during one cycle, leading to less phase shift accumulation. Therefore, a ring cavity has the potential to accommodate a larger phase limitation range and thus has a higher pulse energy generating possibility.

Scaling pulse energy. Based on the above condensed-gain model [53], we went to probe the upper limit of the pulse energy of 2 μm DS fiber lasers. In order to increase the pulse energy, we slightly increased the cavity fiber length, and therefore the pulse repetition rate will decrease and the pulse energy will be enhanced. In addition, we optimize the cavity parameters and manage the intracavity dispersion to scale the pulse energy of DS fiber laser in the 2 μm region. Here, we shorten the gain fiber to an optimal length and at the same time use a short piece of optimized single-mode fiber to compensate the dispersion.
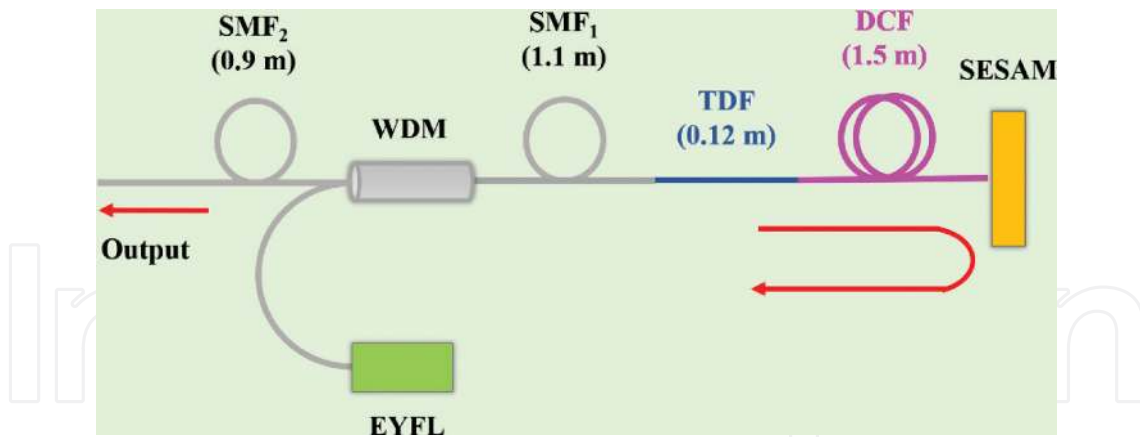
Figure 6. Schematic of the thulium-doped fiber laser passively mode-locked by a semiconductor saturable absorber mirror (SESAM). EYFL, erbium/ytterbium-codoped fiber laser; WDM, wavelength division multiplexer; SMF, single-mode fiber; TDF, thulium-doped fiber; DCF, dispersion-compensating fiber [56].

The experimental system is illustrated in **Figure 6** [56]. Pump light from a continuous-wave (CW) Er/Yb-codoped fiber laser with maximum output of ~1 W centered at 1550 nm was coupled into the fiber through a 1550/1900 nm WDM. The laser cavity includes two pieces of SMF-28 fibers, 12 cm length of single-mode Tm-doped silica fiber (5 µm core and 0.24 NA) and 1.5 m DCF. The DCF was butt coupled to the SESAM, whose reflection combined with the ~4% Fresnel reflection of the perpendicularly cleaved output fiber end completed the laser cavity. The dispersions of the thulium fiber, the SMF-28 fiber, and the DCF at 1920 nm were — 12, −67, and 93 ps²/km, respectively [52], giving a total net cavity dispersion of ~0.004 ps². The SESAM had a relaxation time of 10 ps and a modulation depth of 25%.

When we increased the pump power to 456 mW and at the same time carefully adjusted the SESAM, stable mode-locking was observed and could maintain up to the maximum pump power (1.09 W). Under different pump levels, the average output power was measured, and the pulse energy could be estimated based on the pulsing repetition rate. As shown in **Figure 7**,
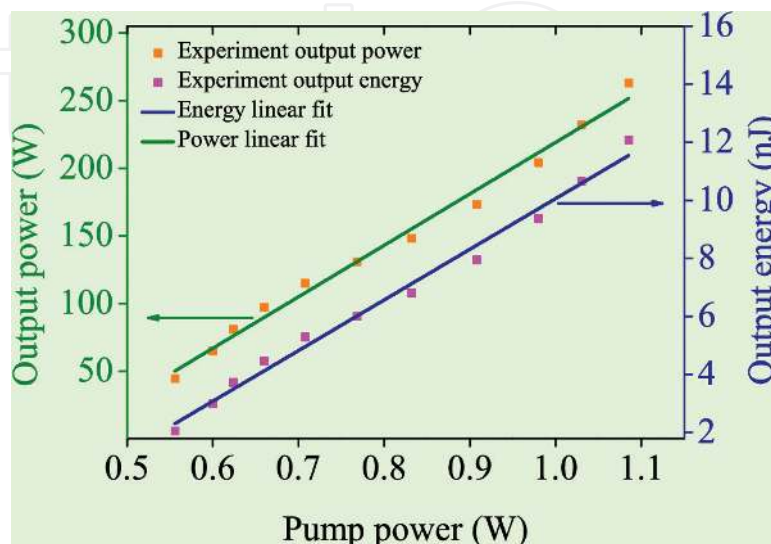

Figure 7. Average output power and pulse energy of the mode-locked fiber laser versus launched pump power [56].

both average power and pulse energy increase near linearly with pump power, and the maximum output power and pulse energy are 263 mW and 12.07 nJ, respectively. **Figure 8** shows the pulse duration versus pump power measured with an autocorrelator. The pulse duration displays a linear increase with pump power, indicating that the pulse was highly chirped. Large chirp is a typical characteristic of DSs for supporting high pulse energy. The laser spectrum, as shown in **Figure 9** [56], locates at 1928.2 nm and has FWHM (full width at half maximum) bandwidth of 2.65 nm. The comparatively narrow spectrum width can be attributed to the high chirp-induced decrease of the pulse peak power. The spectrum shape is very similar to that of another recent report about DS fiber laser at the 1 μm regime [57].

Figure 10(a) shows the pulse train of the mode-locked fiber laser measured at the maximum output level. The pulse train has repetition rate of ~21.8 MHz, consistent with the total
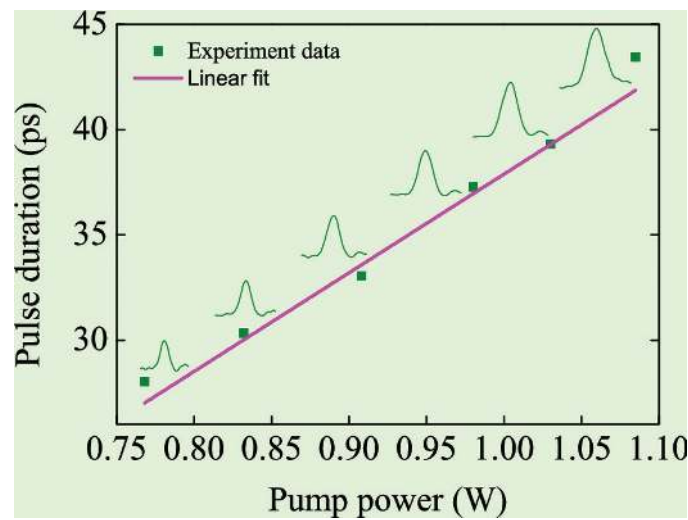

Figure 8. Pulse duration (autocorrelated trace) of the mode-locked fiber laser versus launched pump power [56].
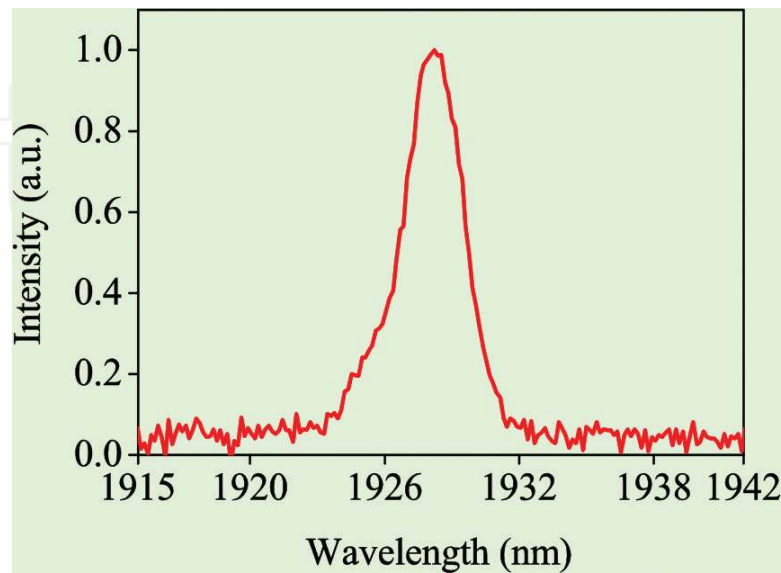

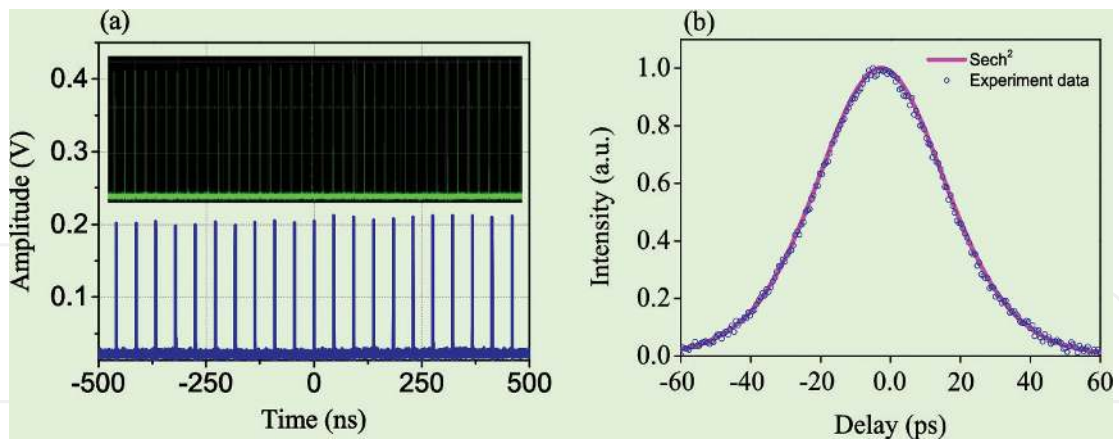**Figure 9.** Laser spectrum of the mode-locked pulse [56].

Figure 10. Dissipative soliton: (a) pulse train on oscilloscope and (b) autocorrelation trace of the single pulse at the maximum output level [56].

cavity length of 4.7 m. **Figure 10(b)** displays the autocorrelation trace of the pulse, giving a FWHM width of 43.5 ps if sech² pulse shape is assumed. Based on the spectral width of 2.65 nm, the pulse has a time-bandwidth product (TBWP) of ~9.3, indicating the presence of large chirp.

4. Dissipative soliton dynamics of 2 µm fiber lasers

The repetition rate of a passively mode-locked fiber laser is usually limited by the total cavity fiber length, and the pulsing repetition rate is generally of several MHz to tens of MHz. However, high-repetition-rate laser pulses are required in some application areas, including biological imaging [58], optical communication [59], and so on. If the high-repetition-rate laser pulses also have high pulse energy, then they are more preferred [60]. There are many ways to generate high-repetition-rate laser pulses from fiber lasers, but the most efficient one may be passive harmonic mode-locking. With harmonic mode-locking, the pulsing frequency will be highly multiplied just through increasing the intracavity light intensity to get higher-order harmonics. However, the single pulse energy usually decreases with increasing harmonic order. The pulse energy of harmonically mode-locked fiber lasers is limited by either pulsing instability or energy storage capability of fibers [61, 62]. In the 2 µm region, passively harmonic mode-locked fiber lasers, especially high-pulse-energy ones, are seldom reported.

Here, based on the CGFML and through appropriate designing the cavity dispersion map and adjusting the cavity gain, we experimentally realize multiple orders of harmonic mode-locking of 2 µm Tm-doped fiber laser (TDFLs) with a SESAM. To achieve high pulse energy, we design this laser to operate in the DS state and adopt a linear laser cavity. We observe stable harmonic mode-locking up to the fourth order, and the pulse energy of all these harmonic pulses is larger than 3 nJ, with the highest one being 12.37 nJ of the fundamental frequency pulsing. Besides harmonic mode-locking, we also observe soliton molecule mode-locking state of this 2 µm DS mode-locked fiber laser.

The laser system we adopted for the passively harmonic mode-locked 2 μm DS fiber laser has a simple configuration, as shown in **Figure 11**. It is mainly consisted of 1.1 m length of standard SMF ($\beta_2 = -67$ ps^2/km), 0.11 m length of thulium-doped fiber ($\beta_2 = -12$ ps^2/km), and 3.5 m length of DCF ($\beta_2 = 93$ ps^2/km). The total cavity net dispersion is estimated to be ~ 0.25 ps^2. A commercial 2 μm SESAM was adopted as the modulator, which has a modulation depth of 25% and relaxation time of 10 ps. A 1.1 W 1550 nm CW Er/Yb-codoped fiber laser was used as the pump source, and a WDM was adopted to launch the pump light into the cavity. The DCF was directly butt coupled to the SESAM. A 0.3-m-long SMF with one end perpendicularly cleaved was employed as the output coupler, and the ~4% fiber facet Fresnel reflection finishes the laser cavity together with the SESAM.

First, we stimulated the laser to operate in the fundamental frequency mode-locking state. This was achieved through increasing the pump power to over a threshold value (here is 456 mW) and at the same time carefully adjusting the position of the SESAM. Once attained, the fundamental frequency mode-locking state could be sustained up to the maximum available pump power (1.1 W). This mode-locking state has a pulse frequency of 21.7 MHz, rightly consistent with the total cavity length of 4.71 m. At the maximum pump level, the average output power was 268 mW, giving a single pulse energy of 12.37 nJ for the fundamental frequency mode-locking.

After accomplishing the fundamental frequency mode-locking, we carefully tuned both the pump power and the SESAM position to achieve higher-order harmonic mode-locking. Here, harmonic mode-locking transition was obtained through changing the intracavity gain, and different light intensity leaded to different pulse dynamics [64]. Harmonic mode-locking from the first to the fourth order was consecutively observed, as presented in **Figure 12** [63]. Compared to the fundamental mode-locking, the pump power had to be increased to over 708 mW to achieve the higher-order harmonic mode-locking. This clearly indicates that more gain is required for sustaining high-order harmonic mode-locking than the fundamental frequency mode-locking. RF spectrum of different harmonic orders at their maximum output powers is shown in **Figure 13**. No clear supermode noise was observed for the fundamental
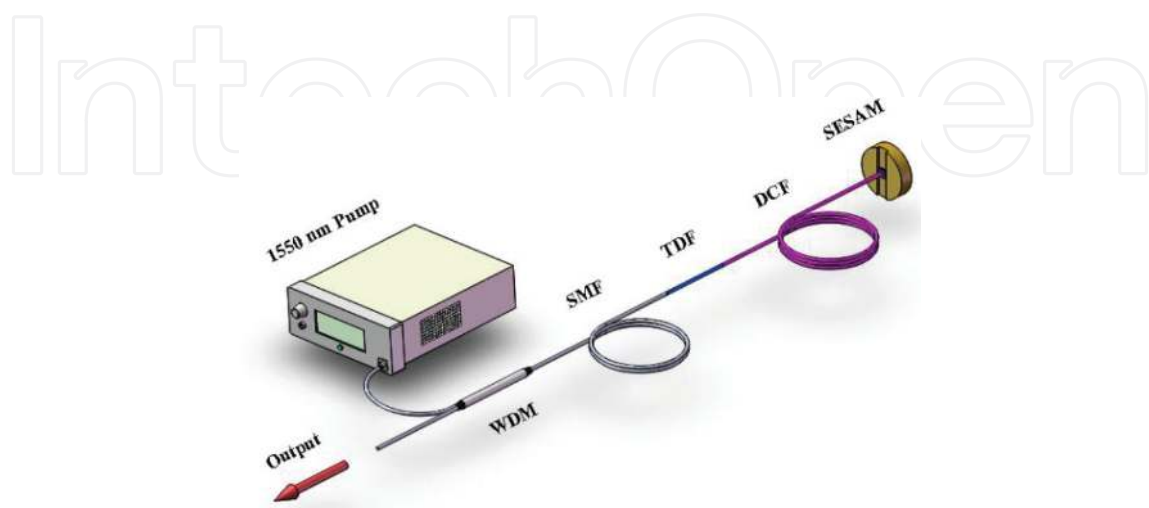

Figure 11. Schematic of the passively mode-locked thulium-doped fiber laser. WDM, wavelength division multiplexer; SMF, single-mode fiber; TDF, thulium-doped fiber; DCF, dispersion-compensating fiber; SESAM, semiconductor saturable absorber mirror [63].
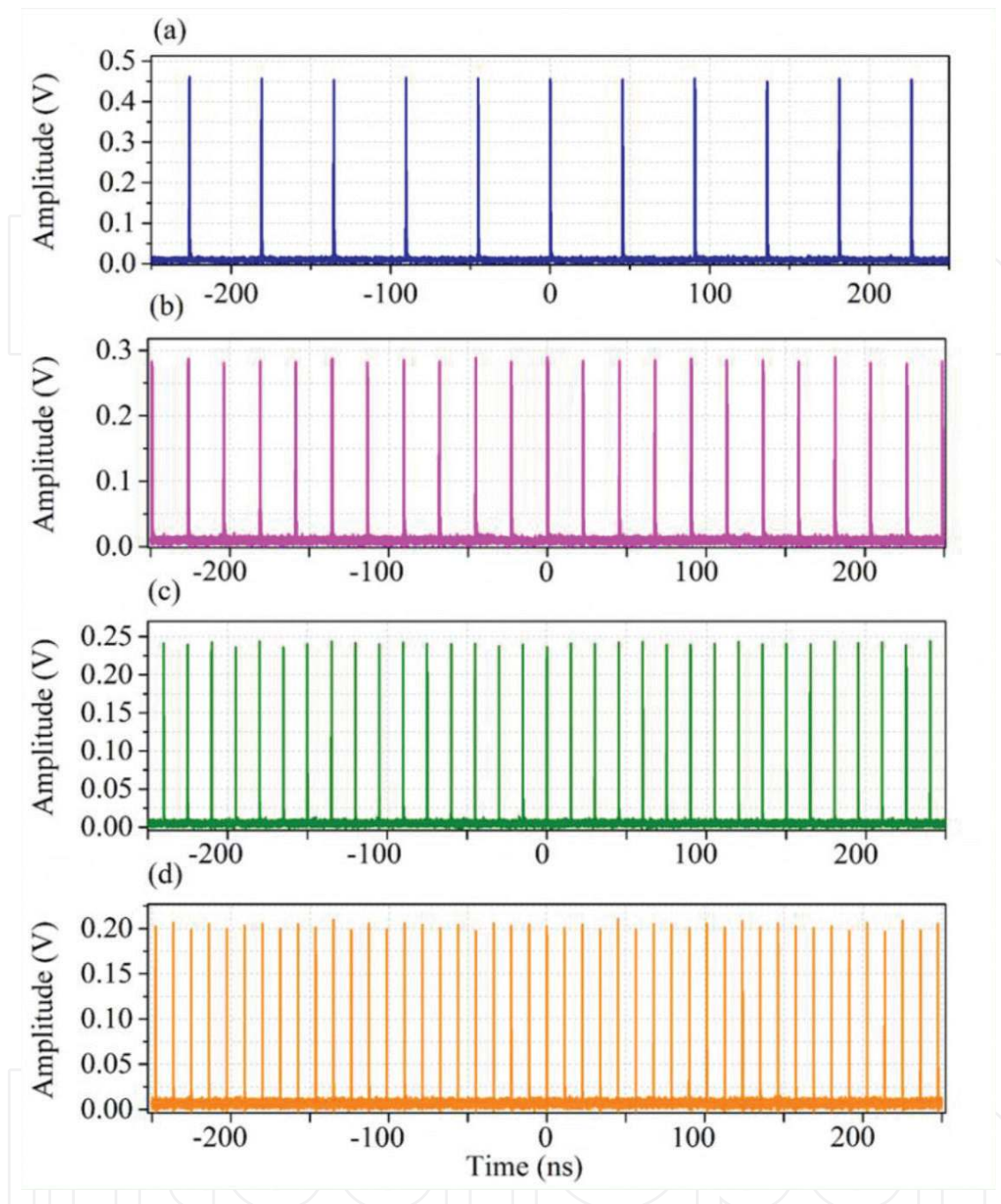
Figure 12. DS pulse trains for (a) fundamental HML at 21.7 MHz, (b) second-order HML at 43.4 MHz, (c) third-order HML at 65.1 MHz, and (d) fourth-order HML at 86.8 MHz [63].

and the fourth harmonics, but certain supermode noises were present for the second and the third harmonics. The SNR for the fourth harmonic mode-locking state is ~38 dB.

Here, the harmonic transfer was achieved through changing the light intensity, which is different from those based on polarization variation [61, 62]. By tuning the SESAM, we change the light spot size incident on the SESAM and therefore change the light intensity and thus nonlinear phase shift. In addition, the cavity loss is also altered through tuning the SESAM. At the appropriate pump level, careful balancing nonlinearity and dispersion, and gain and loss, finally leads to different harmonic mode-locking states.
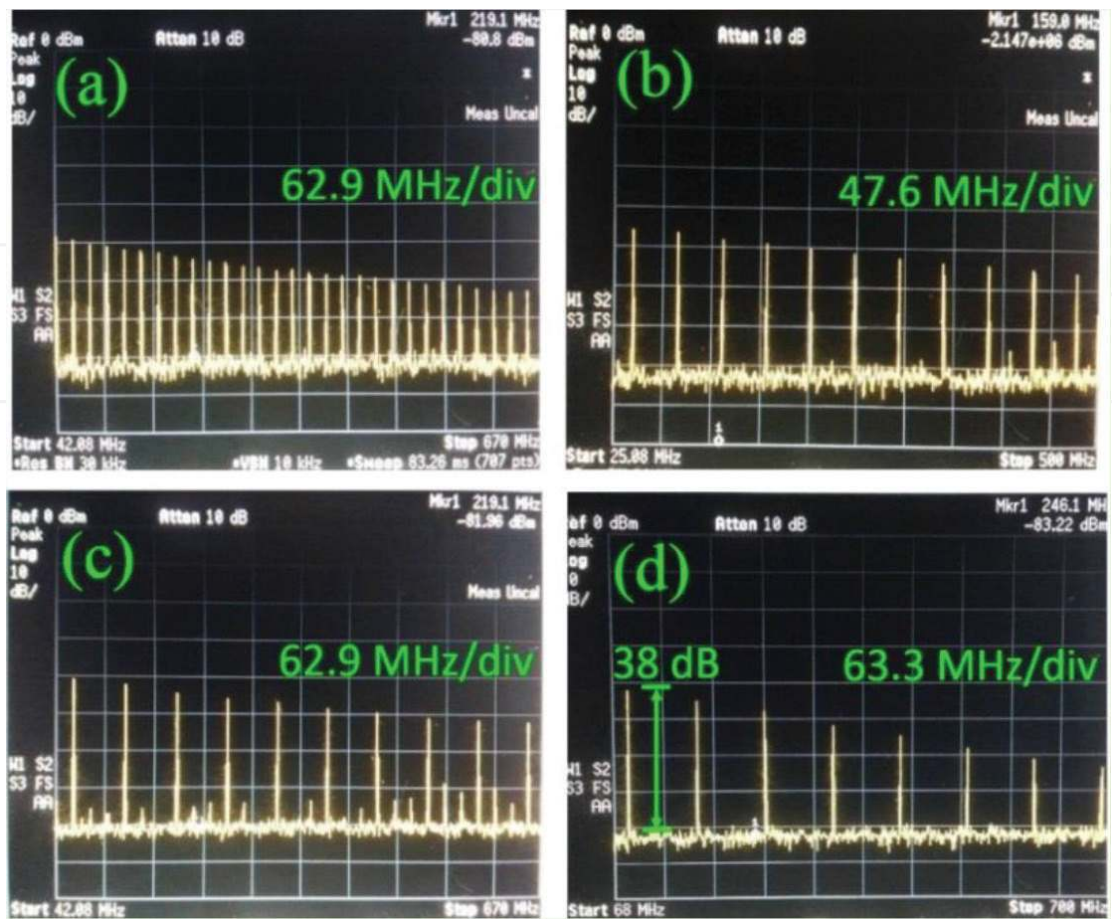
Figure 13. RF spectrum of the fiber laser for the (a) first-, (b) second-, (c) third-, and (d) fourth-order harmonics [63].

In each harmonic mode-locking state, we increased the pump power to the maximum available level, measured the maximum output power, and calculated the corresponding maximum pulse energy, and the results are shown in **Figure 14**. The highest single pulse energy is 12.37 nJ, achieved with the first-order harmonics. With increasing harmonic order, the pulse energy decreases significantly due to that more pulses (every round trip) need to share the laser power. For the fourth-order harmonics, the maximum single pulse energy is 3.29 nJ. We have also observed the sixth- and eighth-order harmonics mode-locking, but they were not stable. This is probably because that the available pump power (thus gain) is not high enough to balance the loss. Therefore, if higher pump power is provided, higher-order 2 μm HML DSs are expected.

Figure 15(a) shows the laser spectrum of the fundamental pulsing and the successive three high-order harmonics measured at their maximum output levels. All these spectra are similar and have a near-triangle shape and center wavelength of 1929 nm. With increasing harmonic order, spectral width tends to narrow a little bit, which is consistent with the theoretical predictions [65] and experimental results [62, 66]. For the first harmonics, the FWHM width is 3.26 nm, while for the fourth harmonics, the FWHM width is decreased to ~2.5 nm. To get more insight of the pulsing characteristics, we measured autocorrelation (AC) traces of both the fundamental mode-locked DSs and high-order harmonics with an autocorrelator. We found that
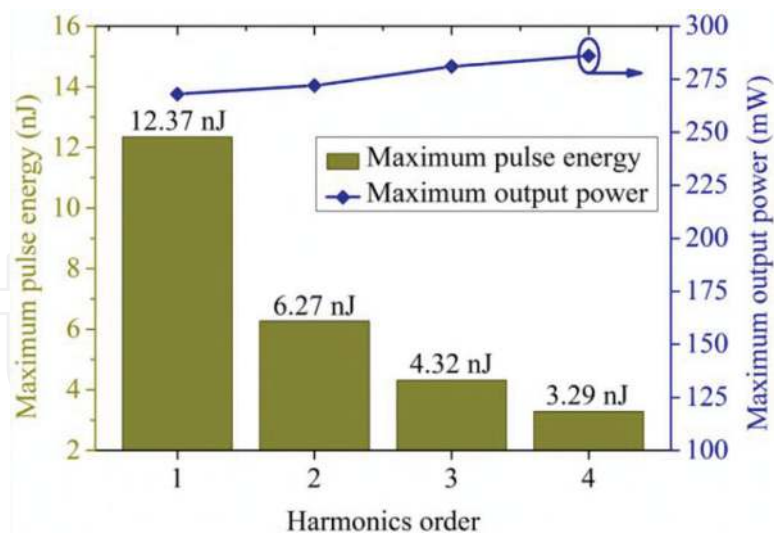
Figure 14. Maximum single pulse energy and average output power of the 2 μm harmonic mode-locked fiber laser at several harmonic orders [63].
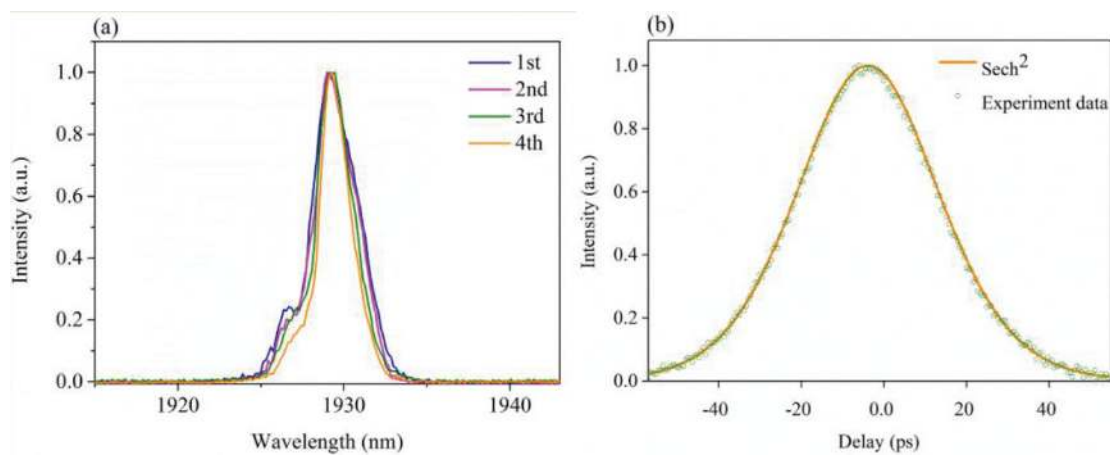

Figure 15. (a) Spectra of the first- to fourth-order harmonic mode-locking solitons and (b) autocorrelation trace of the first-order harmonics [63].

the AC traces of all these harmonics have similar shape and width and the AC of the fundamental mode-locking pulse is present in **Figure 15(b)**. As shown, the AC trace has a FWHM width of 46.37 ps, corresponding to pulse width of ~30 ps when a sech² pulse shape is assumed. For the first-order harmonics (fundamental mode-locking), the time-bandwidth product (TBP) of the pulse is calculated to be close to 8, indicating that the pulse was moderately chirped.

Under every stable mode-locking state, carefully tuning the SESAM can lead to another novel multi-soliton state, the soliton molecule mode-locking. **Figure 16** shows two typical kinds of soliton molecules, doublet and the triplet soliton molecules. Soliton molecule is formed through soliton splitting and strong interaction between separated solitons. The total energy of a soliton molecule entity is proportional to the number of single-soliton constituents [67], but the single-soliton's energy is actually decreased. Under, respectively, maximum pump powers (624 and 660 mW), the output powers of the doublet and the triplet soliton molecules
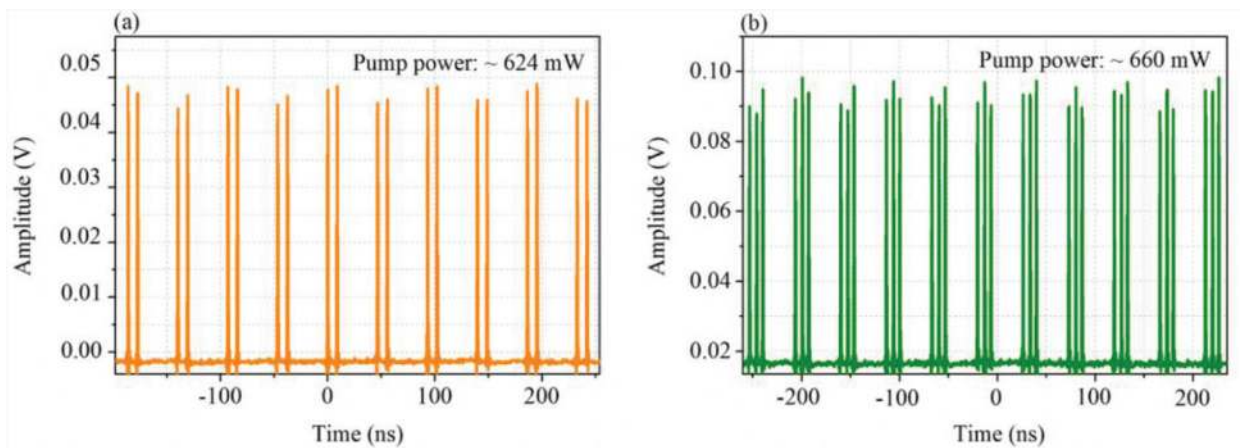
Figure 16. Experimentally measured doublet (a) and triplet (b) soliton molecule pulse trains [63].

are 72 and 95 mW, respectively, corresponding to soliton molecule energies of 3.32 and 4.38 nJ. While their single-soliton energies are 1.66 and 1.46 nJ, respectively.

5. Dissipative soliton 2 μm fiber lasers mode-locked with 2D materials

Although 2 μm Tm[3+]−doped fiber lasers (TDFLs) have valuable applications in sensing, medical surgery, industrial machining, and scientific experiments [68, 69], applications require high-peak-power and/or high-energy laser pulses, which are generally produced by using Q-switching [45, 70] or mode-locking [43, 44] methods. Compared with Q-switching, mode-locking can provide much narrower pulse duration and higher peak power.

Passive mode-locking is usually the preferred choice to get short pulses from 2 μm TDFLs, especially with the maturely developed semiconductor SAs as modulators [47]. However, semiconductor SA has some drawbacks such as complex design and growth procedure [71] and narrow working wavelength range. Recently, graphene (a monolayer of two-dimensional (2D) carbon atoms in a honeycomb structure) has attracted great attention for mode-locking of 2 μm TDFLs [72, 73] due to its advantages of large absorption [74], wide operation spectral range [75], and ultrafast recovery time [76]. Another kind of 2D material MoS_2 has also been extensively explored to mode-lock fiber lasers [57, 77–80]. Although monolayer MoS_2 is a direct band semiconductor (the bandgap determines the energy of photons to be absorbed), studies have proven that layered MoS_2, through introducing stoichiometric defects (non-ideal atomic ratio), also possesses wideband absorption and saturable absorption features [81]. Thereafter, extensive researches have been dedicated to exploring of mode-locking operation and related characteristics of fiber lasers in the 1 μm [57, 77] and 1.5 μm [78–80] wavelength regions. Owing to large anomalous dispersion of the gain fiber and lower absorption of layered MoS_2 at 2 μm, mode-locking operation with this kind of 2D material and corresponding behavior in the 2 μm region still need further verification.

Here, through combining the CGFML and multilayer MoS$_2$, we show that mode-locking capability of layered MoS$_2$ sheets can be definitely extended to the 2 µm wavelength region. With a linear cavity incorporated with the multilayer MoS$_2$ modulator, fundamental mode-locking in the DS regime for 2 µm Tm³⁺ fiber lasers is achieved. At the same time, through elongating the total fiber length, thus decreasing the mode-locking repetition rate, the pulse energy can be scaled to over 15 nJ.

The multilayer MoS$_2$ was synthesized with the liquid-phase exfoliation method (LPE) [6], and the MoS$_2$ nanosheet was transferred onto a gold mirror acting as SA. Raman spectrum of the MoS$_2$ on the mirror was detected with a spectrometer, and the results are shown in **Figure 17(a)**. The spectral position of the E$_{2g}^1$ and A$_{1g}$ modes (~383 cm^{-1} for E$_{2g}^1$ and ~408 cm − 1 for A$_{1g}$) shows that the MoS$_2$ sample has a thickness of approximately four layers [82]. With a self-constructed 1940 nm ~800 ps fiber laser as the probe source, the reflection method was used to measure the saturable absorption of the sample, and the transmittance of the multilayer MoS$_2$ on the gold mirror is shown in **Figure 17(b)** [6]. The nonlinear optical parameters were obtained by using a simple saturable absorption model of [57]

$$T(I) \ = \ 1 - \alpha_0 \times \exp\left(-I/I_{sat}\right) - \alpha_{ns} \tag{4}$$

here, T(I) is the transmission, α_0 is the modulation depth, I is the input intensity, I$_{sat}$ is the saturation intensity, and α_{ns} is the non-saturable absorbance. The measured modulation depth α_0, non-saturable loss α_{ns}, and saturation intensity I$_{sat}$ were 13.6%, 16.7%, and 23.1 MW cm^{-2}, respectively. The modulation depth is comparable to that measured in the 1 µm region [57, 77] but larger than that in the 1.5 µm region [79, 80]. This large modulation depth of the MoS$_2$ SA at the 2 µm wavelength region is efficient for suppressing wave breaking in mode-locking operation [83].
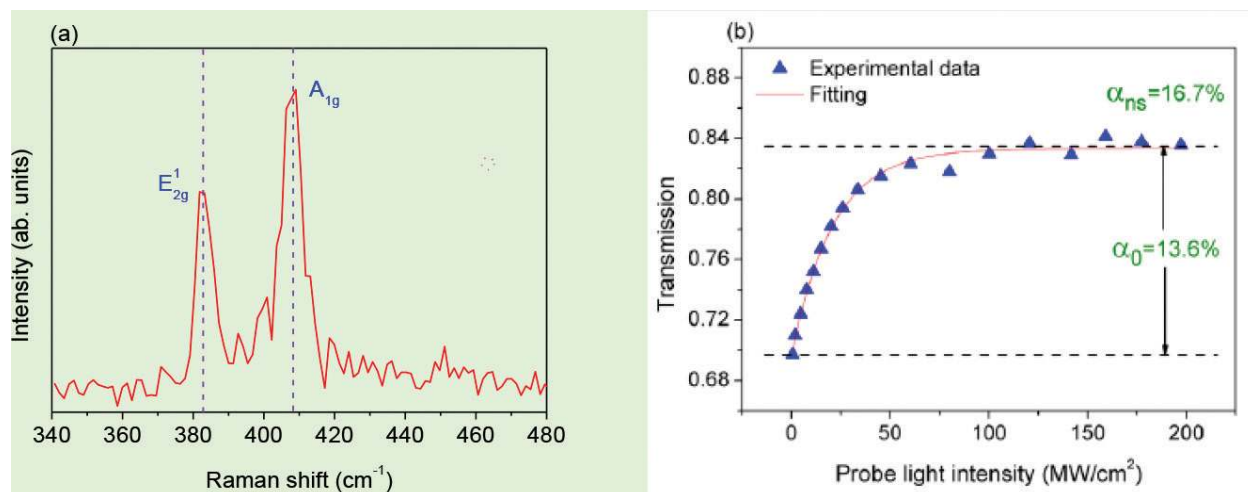

Figure 17. (a) Raman spectrum of the adopted multilayer MoS2 sheets and (b) nonlinear absorption of the multilayer MoS2 sheets coated on a gold mirror [6].

The schematic diagram of the experimental setup for the MoS$_2$ mode-locked TDFL is shown in **Figure 18**. A 1550-nm-CW Er/Yb-codoped fiber laser with maximum output of ~1 W was used as the pump source, and a WDM coupler was used to launch the pump light (with an efficiency of ~95%). The Tm^{3+}-doped silica gain fiber (5/125 μm, 0.24 NA) has core absorption of ~350 dBm^{-1} at ~1550 nm, and 12 cm length of gain fiber was adopted. The dispersion of the gain fiber at 1.9 μm is −12 ps^2 km^{-1}. A 4 m length of SMF-28 fiber was spliced at the output end. To provide normal dispersion, 4.6 m dispersion-compensating fiber (DCF) (2.2 μm, 0.35 NA core) was spliced to the gain fiber. The dispersions of the DCF fiber and the SMF-28 fiber at 1.9 μm are 93 and − 67 ps^2 km^{-1}, respectively [52]. The total net cavity dispersion is ~0.05 ps^2. The DCF fiber was butt coupled to the MoS$_2$ sheet, which was transferred onto a high-reflection gold mirror. High reflection of the gold mirror and the ~3.5% Fresnel reflection of the perpendicularly cleaved output fiber facet completed the laser cavity.

Under pumping, the 2 μm laser first went to CW operation when pump power was over 430 mW. When the pump power was increased to over 630 mW, the laser came to the stable Q-switching regime. Then, further raising the pump power to over 700 mW and careful adjusting the MoS$_2$ position, stable mode-locking operation of the TDFL occurred, which could be sustained up to the available maximum pump power. The output power is linearly dependent on the pump power, and the maximum output power is 150 mW, as shown in **Figure 19** [6]. The slope efficiency is 43.6% with respect to pump power. The laser spectrum of the mode-locked TDFL is centered at ~1905 nm with a FWHM bandwidth of 17.3 nm. This spectral width is much larger than that of the 1 and 1.5 μm counterparts [57, 77–79], showing potential much narrower transform-limited pulse duration of this mode-locked TDFL.

The laser pulse trains obtained at the maximum output level are shown in **Figure 20(a)** [6]. The 103.4 ns period time corresponds well to the cavity round trip time (the total fiber length is ~10 m), showing that the mode-locking operates at the fundamental frequency of 9.67 MHz. The intensity stability between different pulses is >95%. Considering the 150 mW output power, single pulse energy reaches 15.5 nJ. This is the highest pulse energy ever achieved in mode-locked 2 μm fiber lasers with MoS$_2$ modulators, and this also demonstrates that 2D material MoS2 has a great potential in high-power photoelectronics and integrated photonics.

Figure 20(b) displays the single pulse at the maximum power level, which has a Gaussian shape and a FWHM width of 716 ps. This 2 μm DS pulse width is comparable to the 1 μm counterparts [57, 77]. Combined with its spectral width, the 2 μm DS pulse has a time-bandwidth
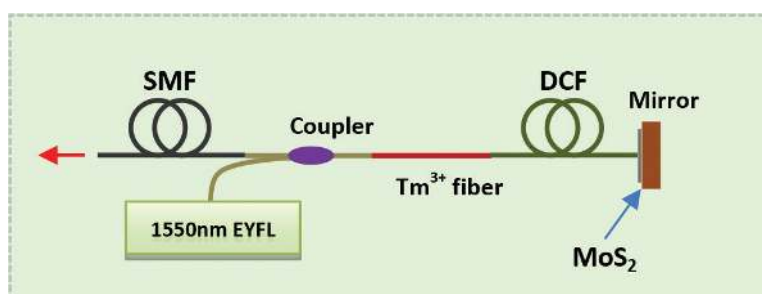

Figure 18. Experimental setup of the mode-locked Tm^{3+} fiber laser. EYFL, erbium/ytterbium-codoped fiber laser; SMF, single-mode fiber; DCF, dispersion-compensating fiber [6].
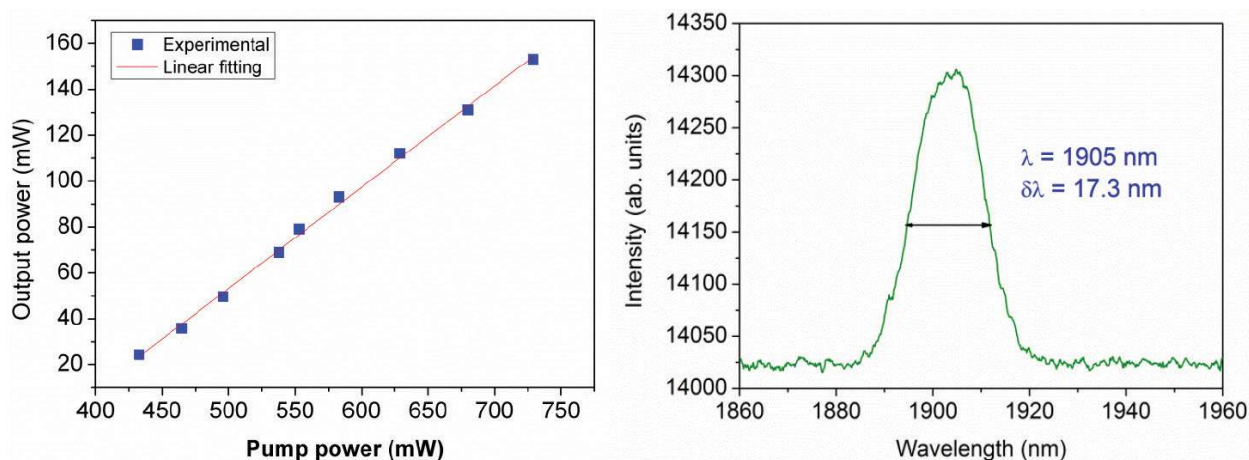
Figure 19. Output (left) and spectrum (right) of the mode-locked Tm³⁺ fiber laser. Square dots are measured data and the solid line is linear fitting [6].

product of ~1200, indicating that the mode-locked laser pulse is highly chirped. Chirping pulse also somehow contributes to high pulse energy. In fact, 2D MoS$_2$ (monolayer or few-layer) has ultrafast recovery times of tens of femtoseconds [84] and ~100 ps [85, 86], corresponding, respectively, to the intraband transition and interband transition of excited free carriers. Recently, mode-locking with similar multilayer MoS$_2$ SAs has achieved femtosecond time-scale pulse durations [79, 80, 87]. Based on the pulse spectral width (17.3 nm) in our experiment, a Fourier transform-limited pulse width of ~247 fs is expected provided that the entire pulse chirp can be compensated.

We also measured the RF spectrum of this MoS$_2$ mode-locked fiber laser, and the RF spectrum (with resolution of 0.1 MHz) is shown in **Figure 21** (left panel). The fundamental pulsing frequency is 9.67 MHz, which is correspondent to the total cavity length. Over the 100 MHz range, no other supermode oscillations are present. The right panel of the figure shows the ninth-order harmonics in a smaller frequency window (20 MHz), and the signal-to-noise ratio is also >40 dB, showing that the MoS$_2$ mode-locked fiber laser is comparatively stable.
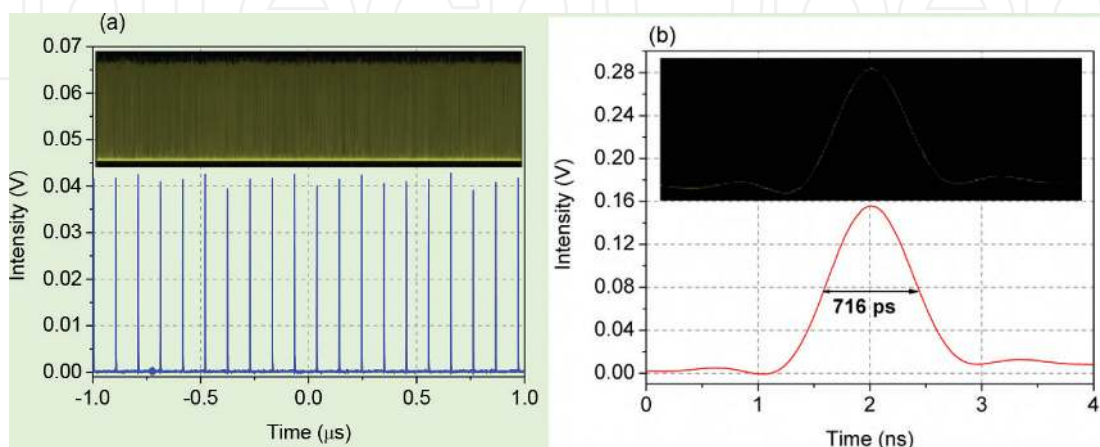

Figure 20. Laser pulse train (a) and single pulse (b) of the MoS2 mode-locked Tm³⁺ fiber laser measured at the maximum output level. Insets show the oscilloscope traces [6].
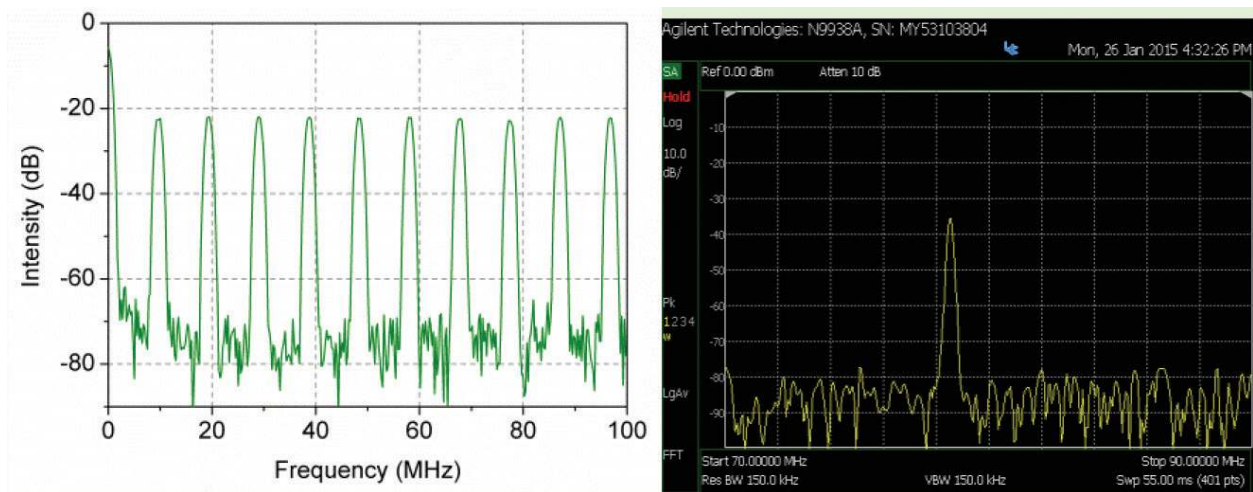
Figure 21. Radiofrequency spectral profile of the mode-locked Tm3+ fiber laser [6].

6. Conclusions and prospects

In recent years, 2 μm fiber lasers with short pulse duration have received great research interests due to great application potentials of 2 μm light sources in areas such as LIDAR, surgical operation, molecule spectroscopy, remote sensing, etc. However, applications usually require high pulse energy, which is hard to achieve with traditional soliton mode-locked fiber lasers. Although various mode-locking mechanisms have been proposed to improve the pulse energy of ultrafast fiber lasers, e.g., dispersion-managed soliton, all normal dispersion mode-locking, self-similar soliton, and dissipative soliton (DS), the pulse energy achieved with 2 μm mode-locked fiber lasers is still much lower than their 1 and 1.5 μm counterparts. This is because that currently available gain fibers and passive fibers are generally anomalous dispersive at 2 μm, which makes mode-locking lie in the traditional soliton regime, and the pulse energy is thus limited by the soliton area theorem clamped by peak power.

DS, based on the balance of both dispersion and nonlinearity and gain and loss, provides a new route to improve the pulse energy of ultrafast fiber lasers. Up to now, pulse energy in 1 and 1.5 μm regions based on DS mode-locking mechanism has been over 20 nJ, giving pulse energies 1~2 orders of magnitude larger than that from conventional soliton mode-locking. However, it is still difficult to generate comparable high energy pulses in 2 μm DS fiber lasers, because of large anomalous dispersion occurred in 2 μm gain fibers.

In order to make advantage of DS mode-locking and improve the pulse energy of 2 μm mode-locked fiber laser, we propose a condensed-gain fiber mode-locking (CGFML), in which the gain fiber should be as short as possible to minimize the nonlinear phase shift caused by the gain fiber. Based on this model, we give detailed exploration of the pulsing dynamics and pulse energy scaling potential of 2 μm thulium-doped mode-locked fiber lasers in several regimes and confirm that this kind of DS mode-locked fiber laser can generate pulse energy over 10 nJ, improving the pulse energy by 1 to 2 orders of magnitude.

In the primary experimental operation based on this model, the 2 μm DS mode-locked Tm-doped fiber laser with a linear cavity delivers 4.9 nJ DSs with pulse duration of 579 fs after being dechirped. Then, through increasing pump power or managing the cavity dispersion map, the pulse energy of this DS fiber is improved to ~12 nJ. We also observe that high-pulse-energy harmonic mode-locked DSs from 2 μm Tm-doped fiber lasers, with single pulse energy of 6.27, 4.32, and 3.29 nJ for the second- to the fourth-order harmonics. Thereafter, DS mode-locking of 2 μm TDFL with 2D material (multilayer MoS$_2$) is investigated, and through decreasing the pulsing frequency, the pulse energy is scaled to 15.5 nJ. This improves the pulse energy of 2 μm mode-locked single-mode fiber lasers to approaching the 1 and 1.5 μm counterparts. All these results show that CGFML DS can be an efficient way to produce high-energy ultrafast pulses from 2 μm TDFLs.

To further scale the pulse energy of the CGFML DS in 2 μm TDFLs, more condensed GFs (which has been available currently) should be adopted, and the total cavity dispersion map should be optimized. Therefore, with higher pump power, more condensed GFs, and further optimized parameters, ultrafast 2 μm pulses with even higher energy are readily feasible.

This CGFML model can be readily extended to beyond 2 μm, e.g., mid-infrared fiber lasers (usually with anomalously dispersive gain media) to scale DS energy and thus is an efficient pulse energy scaling route for anomalous dispersive fiber lasers.

Author details

Yulong Tang*, Chongyuan Huang and Jianqiu Xu

*Address all correspondence to: yulong@sjtu.edu.cn

Key Laboratory for Laser Plasmas (Ministry of Education), Department of Physics and Astronomy, Collaborative Innovation Center of IFSA, Shanghai Jiao Tong University, Shanghai, China

References

[1] Jackson SD. Towards high-power mid-infrared emission from a fibre laser. Nature Photonics. 2012;**6**:423-431

[2] Geng J, Jiang S. The 2 μm market heats up. Optics and Photonics News. 2014;**25**:36-41

[3] Tang Y, Yu X, Li X, Yan Z, Wang QJ. High-power thulium fiber laser Q switched with single-layer graphene. Optics Letters. 2014;**39**:614-617

[4] Wang Y et al. High power tandem-pumped thulium-doped fiber laser. Optics Express. 2015;**23**:2991-2998

[5] Ferman M. E and Hartl I. Nature Photonics. 2013;**7**:868

[6] Tian Z, Wu K, Kong LC, Yang N, Wang Y, Chen R, Hu W, Xu JQ, Tang YL. Lasers Physics Letters. 2015;**12**:065104

[7] Kang K, Liu MY, Gao XJ, Li N, Yin SY, Qin GS, Qin WP. Lasers Physics Letters. 2015;**12**:045106

[8] Xu C, Wise FW. Nature Photonics. 2013;**7**:875

[9] Huang Y, Xu X. Lasers. Physics Letters. 2014;**11**:125101

[10] Matsas VJ, Richardson DJ, Newson TP, Payne DN. Optics Letters. 1993;**18**:358

[11] Honzatko P, Baravets Y, Todorov F. Lasers Physics Letters. 2013;**10**:075103

[12] Xu B, Martinez A, Set SY, Goh CS, Yamashita S. Lasers Physics Letters. 2014;**11**:025101

[13] Gomes LA, Orsila L, Jouhti T, Okhotnikov OG, IEEE J. Selected Topics in Quantum Electronics. 2004;**10**:129

[14] Choudhary A, Lagatsky AA, Zhang ZY, Zhou KJ, Wang Q, Hogg RA, Pradeesh K, Rafailov EU, Sibbett W, Brown CAT, Shepherd DP. Lasers Physics Letters. 2013;**10**:105803

[15] Hasegawa A et al. Transmission of stationary nonlinear optical pulses in dispersion dielectric fibers. I. Anomalous dispersion. Applied Physics Letters. 1973;**23**:142-144

[16] Kelly S. Electronics Letters. 1992;**28**:806

[17] Zakharov V, Shabat A. Soviet Physics JETP. 1973;**37**:823

[18] Tang D Y, Zhao L M, Zhao B and Liu A Q, Physical Review A. 2005;**72**:043816

[19] Wise FW, Chong A, Renninger WH. High-energy femtosecond fiber lasers based on pulse propagation at normal dispersion. Laser & Photonics Review. 2008;**2**:58-73

[20] Tamura K, Ippen EP, Haus HA, Nelson LE. 77-fs pulse generation from a stretched-pulse mode-locked all-fiber ring laser. Optics Letters. 1993;**18**:1080-1082

[21] Tamura K, Ippen EP, Haus HA. Pulse dynamics in stretched-pulse fiber lasers. Applied Physics Letters. 1995;**67**:158-160

[22] Lim H, Ilday FO, Wise FW. Femtosecond ytterbium fiber laser with photonic crystal fiber for dispersion control. Optics Express. 2002;**10**:1497-1502

[23] Ilday FO, Wise FW. Nonlinearity management: A route to high-energy soliton fiber lasers. Journal of Optical Society America B. 2002;**19**:470-476

[24] Tang DY, Zhao LM, Xie GQ, Qian LJ. Coexistence and competition between different soliton-shaping mechanisms in a laser. Physical Review A. 2007;**75**:063810

[25] Ilday FO, Buckley JR, Lim H, Wise FW, Clark WG. Generation of 50-fs, 5-nJ pulses at 1.03 μm from a wave-breaking free fiber laser. Optics Letters. 2003;**28**:1365-1367

[26] Buckley JR, Wise FW, Ilday FO, Sosnowski T. Femtosecond fiber lasers with pulse energies above 10 nJ. Optics Letters. 2005;**30**:1888-1890

[27] Ilday FO, Buckley JR, Clark WG, Wise FW. Self-similar evolution of parabolic pulses in a laser. Physical Review Letters. 2004;**92**:213902

[28] Renninger WH, Chong A, Wise FW. Self-similar pulse evolution in an all-normal-dispersion laser. Physical Review A. 2010;**021805**(R):82

[29] Liu H, Liu Z, Lamb ES, Wise F. Self-similar erbium-doped fiber laser with large normal dispersion. Optics Letters. 2014;**39**:1019-1021

[30] Oktem B, Ulgudur C, Ilday FO. Soliton-similariton fibre laser. Nature Photonics. 2010;**4**:307-311

[31] Chong A, Renninger WH, Wise FW. All-normal-dispersion femtosecond fiber laser. Optics Express. 2006;**14**:10095-10100

[32] Chong A, Renninger WH, Wise FW. Properties of normal-dispersion femtosecond fiber lasers. Journal of the Optical Society of America B: Optical Physics. 2008;**25**:140-148

[33] Chong A et al. All-normal-dispersion femtosecond fiber laser with pulse energy above 20 nJ. Optics Letters. 2007;**32**:2408-2410

[34] Kieu K, Renninger WH, Chong A, Wise FW. Sub-100 fs pulses at wattlevel powers from a dissipative-soliton fiber laser. Optics Letters. 2009;**34**:593-595

[35] Chichkov NB et al. High-power dissipative solitons from an all-normal dispersion erbium fiber oscillator. Optics Letters. 2010;**35**:2807-2809

[36] Bale B, Boscolo S, Turitsyn S. Dissipative dispersion-managed solitons in mode-locked lasers. Optics Letters. 2009;(21):3286-3288

[37] Renninger WH, Wise FW. IEEE Journal of Selected Topics in Quantum Electronics. 2015;**21**:101

[38] Chichkov NB, Hapke C, Neumann J, Kracht D, Wandt D, Morgner U. Optics Express. 2012;(4):3844

[39] Zhao LM, Tang DY, Wu J. Optics Letters. 2006;**31**:1788

[40] Baumgartl M, Ortaç B, Lecaplain C, Hideur A, Limpert J, Tünnermann A. Optics Letters. 2010;**35**:2311

[41] Mao D, Liu XM, Wang RL, Hu XH, Lu H. Laser Physics Letters. 2011;**8**:134

[42] Choi SY, Jeong H, Hong BH, Rotermund F, Yeom D. Laser Physics Letters. 2014;**11**:015101

[43] Nelson LE, Ippen EP, Haus HA. Broadly tunable sub-500 fs pulses from an additive-pulse mode-locked thulium-doped fiber ring laser. Applied Physics Letters. 1995;**67**:19-21

[44] Sharp RC, Spock DE, Pan N, Elliot J. 190-fs passively mode-locked thulium fiber laser with a low threshold. Optics Letters. 1996;**21**:881-883

[45] Solodyankin MA et al. Mode-locked 1.93 μm thulium fiber laser with a carbon nanotube absorber. Optics Letters. 2008;**33**:1336-1338

[46] Wang Q, Geng J, Luo T, Jiang S. Mode-locked 2 µm laser with highly thulium-doped silicate fiber. Optics Letters. 2009;**34**:3616-3618

[47] Wang Q, Geng J, Jiang Z, Luo T, Jiang S. Mode-locked tm–Ho-codoped fiber laser at 2.06 µm. IEEE Photonics Technology Letters. 2011;**23**:682-684

[48] Wang Q, Chen T, Zhang B, Heberle AP, Chen KP. All-fiber passively mode-locked thulium-doped fiber ring oscillator operated at solitary and noiselike modes. Optics Letters. 2011;**36**:3750-3752

[49] Gumenyuk R, Vartiainen I, Tuovinen H, Okhotnikov OG. Dissipative dispersion-managed soliton 2 µm thulium/holmium fiber laser. Optics Letters. 2011;**36**:609-611

[50] Agrawal GP. Nonlinear Fiber Optics. Academic Press; 2007

[51] Haxsen F, Wandt D, Morgner U, Neumann J, Kracht D. Monotonically chirped pulse evolution in an ultrashort pulse thulium-doped fiber laser. Optics Letters. 2012;**37**:1014-1016

[52] Wang QQ et al. All-fiber ultrafast thulium-doped fiber ring laser with dissipative soliton and noise-like output in normal dispersion by single-wall carbon nanotubes. Applied Physics Letters. 2013;**103**:011103

[53] Huang C, Wang C, Shang W, Tang Y, Xu J. Scientific Reports. 2015;**5**:13680

[54] Renninger WH, Wise FW. Pulse shaping and evolution in normal-dispersion mode-locked fiber lasers. IEEE Journal of Selected Topics in Quantum Electronics. 2012;**18**:389-398

[55] Cabasse A. 130 mW average power, 4.6 nJ pulse energy, 10.2 ps pulse duration from an Er3+ fiber oscillator passively mode locked by a resonant saturable absorber mirror. Optics Letters. 2011;**36**:2620-2622

[56] Yang N, Huang CY, Tang Y, Xu J. Lasers Physics Letters. 2015;**055101**:12

[57] Du J, Wang Q, Jiang G, Xu C, Zhao C, Xiang Y, Chen Y, Wen S, Zhang H. Scientific Reports. 2014;**4**:6346

[58] Chu SW, Chen SY, Tsai TH, Liu TM, Lin CY, Tsai HJ, Sun CK. Optics Express. 2003;**11**:3093

[59] Yilmaz T, Depriest CM, Turpin T, Abeles JH, Delfyett PJ. IEEE Photonics Technology Letters. 2002;**14**:1608

[60] Richardson DJ, Nilsson J, Clarkson WA. Journal of the Optical Society of America B: Optical Physics. 2010;**27**:B63

[61] Yan PG, Lin RY, Ruan SC, Liu AJ, Chen H. Optics Express. 2015;**23**:154

[62] Peng JS, Zhan L, Luo SY, Shen QS. Journal of Lightwave Technology. 2013;**31**:3009

[63] Yang N, Tang YL. Xu J, Lasers. Physics Letters. 2015;**12**:085102

[64] Kutz JN, Sandtede B. Optics Express. 2008;**16**:636

[65] Haboucha A, Komarov A, Leblond H, Sanchez F, Martel G. Optical Fiber Technology. 2008;**14**:262

[66] Chen H, Chen SP, Jiang ZF, Hou J. Optics Express. 2015;**23**:1308

[67] Akhmediev N, Grelu P. Nature Photonics. 2012;**6**:84

[68] Zhang Y, Tian Y, Wang W, Yao B. Tunable narrow linewidth Tm3+–doped silica fiber laser with an intracavity taper. Laser Physics Letters. 2010;**7**:225

[69] Wang F, Shen DY, Fan DY, Lu QS. High power widely tunable Tm3+: Fiber laser with spectral linewidth of 10 pm. Laser Physics Letters. 2010;**7**:450

[70] Eichhorn M, Jackson SD. High-pulse-energy actively Q-switched Tm3+–doped silica 2 µm fiber laser pumped at 792 nm. Optics Letters. 2007;**32**:2780

[71] Saraceno CJ, Schriber C, Mangold M, Hoffmann M, Heckl OH, Baer CRE, Golling M, Südmeyer T, Keller U. SESAMs for high-power oscillators: Design guidelines and damage thresholds. IEEE Journal of Selected Topics in Quantum Electronics. 2012;**18**:29

[72] Sobon G, Sotor J, Pasternak I, Krajewska A, Strupinski W, Abramski KM. Thulium-doped all-fiber laser mode-locked by CVD-graphene/PMMA saturable absorber. Optics Express. 2013;**21**:12797

[73] Wang Q, Chen T, Zhang B, Li M, Lu Y, Chen KP. All-fiber passively mode-locked thulium-doped fiber ring laser using optically deposited graphene saturable absorbers. Applied Physics Letters. 2013;**102**:131117

[74] Nair RR, Blake P, Grigorenko AN, Novoselov KS, Booth TJ, Stauber T, Peres NMR, Geim AK. Fine structure constant defines visual transparency of grapheme. Science. 2008;**320**:1308

[75] Zhang YZ, Liu T, Li XH, Liang G, Meng B, Hu X, Wang QJ". Broadband high photoresponse from pure monolayer graphene-based photodetector. Nature Communications. 2013;**4**:1811

[76] Bao Q, Zhang H, Wang Y, Ni Z, Yan Y, Shen ZX, Loh KP, Tang DY. Atomic-layer graphene as a saturable absorber for ultrafast pulsed lasers. Advanced Functional Materials. 2009;**19**:3077

[77] Zhang H, Lu SB, Zheng J, Du J, Wen SC, Tang DY, Loh KP. Molybdenum disulfide (MoS2) as a broadband saturable absorber for ultra-fast photonics. Optics Express. 2014;**22**:7249

[78] Xia H, Li H, Lan C, Li C, Zhang X, Zhang S, Liu Y. Ultrafast erbium-doped fiber laser mode-locked by a CVD grown molybdenum disulfide (MoS2) saturable absorber. Optics Express. 2014;**22**,17341

[79] Liu H, Luo A, Wang F, Tang R, Liu M, Luo Z, Xu W, Zhao C, Zhang H. Femtosecond pulse erbium-doped fiber laser by a few-layer MoS2 saturable absorber. Optics Letters. 2014;**39**:4591

[80] Khazaeizhad R, Kassani SH, Jeong H, Yeom D, Oh K. Mode-locking of Er-doped fiber laser using a multilayer MoS2 thin film as a saturable absorber in both anomalous and normal dispersion regimes. Optics Express. 2014;**22**,23732

[81] Wang S, Yu H, Zhang H, Wang A, Zhao M, Chen Y, Mei L, Wang J. Broadband few-layer MoS2 saturable absorbers. Advanced Materials. 2014;**26**:3538

[82] Li H, Zhang Q, Yap CCR, Tay BK, Edwin THT, Olivier A, Baillargeat D. From bulk to monolayer MoS2:Evolution of Raman scattering. Advanced Functional Materials. 2012;**22**:1385

[83] Cabasse A, Martel G, Oudar JL. High power dissipative soliton in an erbium-doped fiber laser modelocked with a high modulation depth saturable absorber mirror. Optics Express. 2009;**17**:9537

[84] Wang K et al. Ultrafast saturable absorption of 2D MoS2 nanosheets. ACS Nano. 2013;**7**:9260

[85] Korn T, Heydrich S, Hirmer M, Schmutzler J, Schuller C. Low-temperature photocarrier dynamics in monolayer MoS2. Applied Physics Letters. 2011;**99**:102109

[86] Wang R, Ruzicka BA, Kumar N, Bellus MZ, Chiu HY, Zhao H. Ultrafast and spatially resolved studies of charge carriers in atomically thin molybdenum disulphide. Physical Review B. 2012;**86**:045406

[87] Wu K, Zhang X, Wang J, Chen J. 463 MHz fundamental mode-locked fiber laser based on few-layer MoS2 saturable absorber. Optics Letters. 2015;**40**:1374